Molecular Crystals and Liquid Crystals Science and Technology. Section A. Molecular Crystals and Liquid Crystals
Publication details, including instructions for authors and subscription information:
http://www.tandfonline.com/loi/gmcl19

Motion and Disorder in the Plastic Crystal of the C_{70} Complex with Toluene by Solid State NMR and Thermal Analysis

J. Cheng [a b], Y. Jin [a b], A. Xenopoulos [a b], W. Chen [a b], B. Wunderlich [a b], M. Diack [a b], R. N. Compton [a b] & G. Guiochon [a b]

[a] Chemistry Division, Oak Ridge National Laboratory, Oak Ridge, Tennessee, 37831-6197
[b] Department of Chemistry, The University of Tennesee, Knoxville, Tennessee, 37996-1600

Version of record first published: 24 Sep 2006.

To cite this article: J. Cheng , Y. Jin , A. Xenopoulos , W. Chen , B. Wunderlich , M. Diack , R. N. Compton & G. Guiochon (1994): Motion and Disorder in the Plastic Crystal of the C_{70} Complex with Toluene by Solid State NMR and Thermal Analysis, Molecular Crystals and Liquid Crystals Science and Technology. Section A. Molecular Crystals and Liquid Crystals, 250:1, 359-371

To link to this article: http://dx.doi.org/10.1080/10587259408028220

Mol. Cryst. Liq. Cryst., 1994, Vol. 250, pp. 359–371
Reprints available directly from the publisher
Photocopying permitted by license only

Printed in the United States of America

Motion and Disorder in the Plastic Crystal of the C_{70} Complex with Toluene by Solid State NMR and Thermal Analysis

J. CHENG, Y. JIN, A. XENOPOULOS, W. CHEN, B. WUNDERLICH,*
M. DIACK, R. N. COMPTON and G. GUIOCHON

Chemistry Division, Oak Ridge National Laboratory, Oak Ridge, Tennessee 37831-6197 and Department of Chemistry, The University of Tennessee, Knoxville, Tennessee 37996-1600

(Received June 11, 1993; in final form October 12, 1993)

Molecular motion and disorder in a C_{70} toluene complex of molar ratio 1/1 have been analyzed by obtaining ^{13}C NMR powder patterns and magic angle spinning spectra over the temperature range from 150 to 373 K, as well as by DSC measurement of heat capacity and heats of transition from 120 to 560 K. The C_{70} molecules start some orientational motion below 150 K. The well-known transitions of C_{70} between 260 and 350 K are suppressed in the complex, but the toluene molecules contribute a liquid-like heat capacity above 178 K. Evaporation of the toluene occurs sharply at 446 K with a heat of decomposition of 36.1 kJ/mol (2.9 kJ/mol more than the heat of evaporation of pure toluene and 62 K higher than the boiling temperature of toluene). At room temperature and above, pure C_{70} has a rotational correlation time of less than 100 μs, while for the toluene-containing C_{70} the motion is much less. The toluene molecules are closer to the equatorial "belt" of the C_{70} prolate spheroid and prohibit the C_{70} molecules from rotating isotropically.

Keywords: C_{70} complex with toluene, motion, disorder, crystal, plastic crystal, solid state NMR, thermal analysis, heat capacity.

INTRODUCTION

Following our previous work on C_{60}[1] and C_{70},[2] we are presenting here the characterization of the 1:1 C_{70} complex with toluene ($C_{70}\cdot C_6H_5CH_3$). Differential scanning calorimetry (DSC) on C_{70} shows two reproducible transitions and a broad increase in heat capacity, signaling beginning disorder and motion at lower temperatures.[2] Above the transition temperatures both carbon allotropes are thus plastic crystals. Solvent is retained by C_{70} to a much larger extent than by C_{60}. Combining DSC with mass spectrometry showed that a sharp endotherm of C_{70} precipitated from toluene in the range 395 to 445 K, to be analyzed below, can be attributed to decomposition of a C_{70}·toluene complex. This endotherm was earlier reported by Grivei *et al.* and Vaughan *et al.*, but not analyzed in detail.[3] We have established the composition by weight-loss on decomposition and purity of the substances by NMR and mass spectrometry to be about 98%.

Investigations of solid state ^{13}C NMR on C_{70} have to date only been carried out at room temperature.[4,5] These reports show that at room temperature, C_{70} molecules in either their pure form or in a mixture with C_{60} exhibit substantial orientational motion. In order to understand the dynamics and phase transitions, it is, however, necessary to

study the molecular motion over a wider range of temperature. Thus, in this paper, variable-temperature solid-state ^{13}C NMR data are presented for both, C_{70} and the complex to elucidate the motion and disorder that causes the observed phase transitions.

The ^{13}C NMR observations in this paper focus on the molecular motion and orientational disorder of the C_{70} molecules in the presence of toluene (as-received sample). The pure C_{70} was obtained after decomposition of the complex at 473 K and was analyzed for comparison to provide information on the function of the toluene molecules in hindering the motion of C_{70}. The molecular motion is followed by observations of the reduction of the linewidth of the powder spectrum. The participation of toluene molecules in the crystallization of C_{70} is identified by the ^{13}C cross-polarization and magic-angle-spinning (CP-MAS) spectrum of C_{70} molecules. The prediction that the toluene molecules occupy spaces with octahedral coordination of the C_{70} lattice can be rationalized based on the one-to-one molar ratio of C_{70}/toluene and the cross-polarization behavior.

EXPERIMENTAL

Sample

The sample of C_{70} was isolated from soot, as described in the previous paper.[2] The fullerenes were then extracted using boiling toluene.

In spite of chromatographic purification (see Reference 2), the as-received sample of C_{70} still contains toluene to a much larger extent than a similarly purified C_{60}. For the particular sample used in this study, the presence of toluene can be identified by the solid state ^{13}C NMR spectra which will be shown and discussed in detail in the Results and Discussion. After heating at 10 K/min to above 473 K, the sample shows no NMR resonances from toluene molecules, and has a mass loss of $(9.6 \pm 0.5)\%$, corresponding to the loss of one toluene per C_{70} (calculated loss 9.88%). Thus, the molar ratio between C_{70} and toluene in the as-received sample could be determined to be close to 1:1. The total amount of C_{70} used for any NMR or DSC measurement was about 10 mg, and for DSC analysis was 20–30 mg. Pure C_{70} (proven by mass spectrometry) was produced by preheating to 473 K.

^{13}C NMR

The ^{13}C NMR experiments were performed on a modified Nicolet NT 200 spectrometer, operating at 50.31 MHz for ^{13}C. The standard 5 mm magic-angle-spinning (MAS) probe was purchased from Doty. The sample rotor is made from sapphire (Al_2O_3) and the end caps are made from Kel-F, polychlorotrifluoroethylene (—CClF—CF_2). In most measurements the pulse sequence used is the conventional single pulse experiment without decoupling of protons. An independent run of the empty rotor with Kel-F end caps showed no detectable signals with 6000 scans, which is the typical number of transients accumulation in this work. The spectral window is 10,000 Hz. Data size for the free induction decay is 8 kbytes. To detect the existence and

behavior of toluene molecules in the as-received sample, the cross-polarization and magic angle spinning (CP-MAS) techniques were applied. The contact time was 1.2 ms, recycle time was 3 s, and the 90°-pulse width for protons was 5.0 μs.

Calorimetry

A commercial Thermal Analyst 2100 system from TA Instruments Inc. with a 912 dual sample DSC and DSC auto-sampler were used for heat capacity transition measurements. All heat capacities were measured at 10 K/min heating rate with N_2 gas flow of 10 mL/min above 300 K, and with stationary N_2 gas below 300 K. Precision, calibration and mode of operation is discussed in the previous paper.[2]

RESULTS

Calorimetry

The heat capacity of the as-receive sample ($C_{70}\cdot C_7H_5CH_3$) was measured first from 120 to 370 K, just below the boiling point of toluene (383.7 K, heat of evaporation 33.2 kJ/mol). The results are shown in Figure 1, curve A. A shallow, broad endotherm is visible from 170 to 280 K and is still present after the sample was cooled from 370 K and reheated (curve B). The mass loss in the first heating was less than 1%. Heating the sample further to 470 K shows two endotherms: one is very small, with a transition enthalpy of 1.124 J/g at 390.3 K (onset) or 397.1 K (peak), and the other is quite large

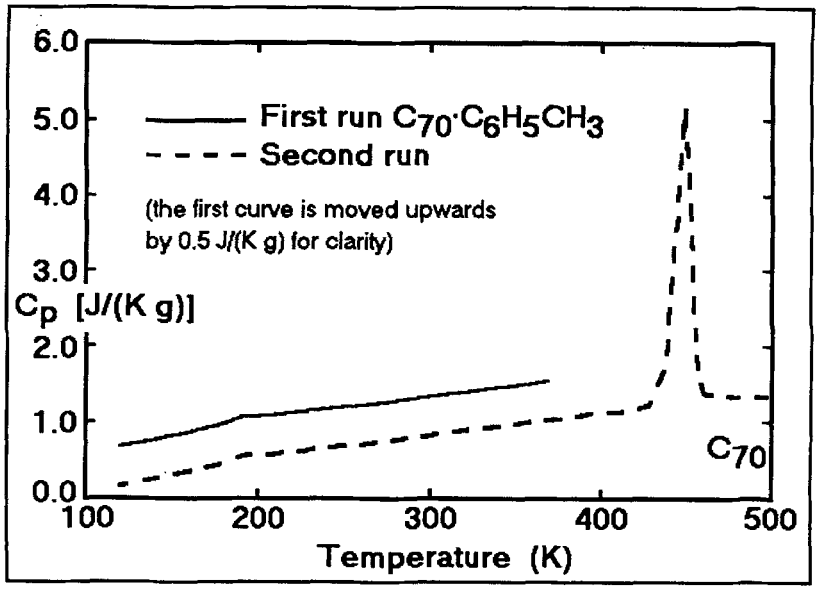

FIGURE 1 Heat capacities of the as-received sample. A. First heating to 370 K (upper curve). B. Second heating (lower curve). Curve A is moved upwards by 0.5 $JK^{-1}g^{-1}$ for clarity.

TABLE I

Heat Capacity of the $C_{70}\cdot C_6H_5CH_3$ Complex, Toluene and C_{70} in the Complex in J/G

T(K)	$C_{70}\cdot C_6H_5CH_3$	Toluene[a]	C_{70}[b]
120.00	0.187	0.745	0.127
130.00	0.222	0.779	0.163
140.00	0.271	0.813	0.214
150.00	0.323	0.850	0.267
160.00	0.370	0.890	0.315
170.00	0.416	0.935	0.361
180.00	0.477	1.471	0.371
190.00	0.561	1.477	0.464
200.00	0.580	1.487	0.483
210.00	0.595	1.499	0.499
220.00	0.628	1.515	0.534
230.00	0.659	1.533	0.566
240.00	0.683	1.552	0.591
250.00	0.705	1.575	0.613
260.00	0.722	1.599	0.629
270.00	0.758	1.625	0.666
273.15	0.767	1.633	0.675
280.00	0.783	1.652	0.691
290.00	0.814	1.682	0.722
298.15	0.834	1.706	0.742
300.00	0.841	1.712	0.749
310.00	0.874	1.744	0.781
320.00	0.909	1.776	0.816
330.00	0.938	1.810	0.845
340.00	0.972	1.843	0.879
350.00	1.000	1.875	0.907
360.00	1.028	1.910	0.934
370.00	1.055	1.942	0.961
380.00	1.083	1.975	0.988
390.00	1.115	2.008	1.020
400.00	1.155	2.041	1.061
410.00	1.166	2.074	1.070
420.00	1.201	2.107	1.105
430.00	1.260	2.140	1.167
440.00	1.808	2.173	1.770
450.00	5.179	2.206	5.495
460.00	1.258	2.239	1.258
470.00	1.219	2.272	1.219
480.00	1.205	2.305	1.205
490.00	1.212	2.338	1.212
500.00	1.218	2.371	1.218

[a] Data refer to the liquid toluene above the melting temperature of pure toluene (178 K). Data above the boiling point (384 K) were extrapolated based on the equation $C_p = 0.1723 + 0.0007888^* T$ (J/g) ($T > 360$ K). Below the melting point, the toluene data refer to the solid state. Above the decomposition, no toluene correction was done.

[b] Calculated using the equation $C_{70} =$ [Complex − (Toluene × 0.096)]/(0.904) before decomposition of the complex $C_{70}\cdot C_6H_5CH_3$ at 452 K.

with a transition enthalpy of 37.6 J/g (36.1 kJ/mol) at 445.7 K (onset) or 452.0 K (peak). The weight loss after this run was 9.6% as outlined above and was rationalized to correspond to the loss of one toluene per C_{70}. Since the boiling point of toluene is 383.7 K, the small transition at 397 K may relate to the evaporation of a small amount of excess toluene, while the large transition at higher temperature is the decomposition

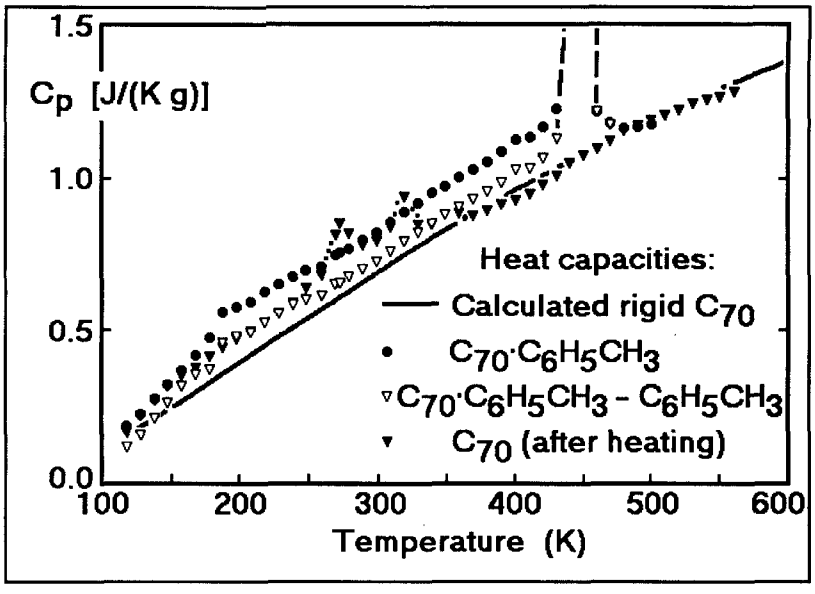

FIGURE 2 Experimental heat capacities of $C_{70}\cdot C_6H_5CH_3$ (filled circles), C_{70} (filled triangles and dotted line in the transition area), and the calculated vibration only heat capacity of C_{70} (solid line). The additional open triangles represent the heat capacity of C_{70} in the complex, computed as shown in Table I.

of the $C_{70}\cdot C_6H_5CH_3$ complex. The energy required to break the complex is the difference between the measured endotherm and the heat of evaporation of liquid toluene, $36.1 - 33.2 = 2.9$ kJ/mol. The heat capacity of $C_{70}\cdot C_6H_5CH_3$ is listed in Table I.

After the sample was pretreated at 473 K, the low temperature, broad transition disappeared, while three new transitions, characteristic of pure C_{70}, developed from 250 to 380 K. Their temperatures, enthalpies and entropies of transitions are discussed in Reference 2. Also given in Reference 2 is the discussion of the heat capacity of C_{70}.

Figure 2 shows the measured heat capacities of $C_{70}\cdot C_6H_5CH_3$ (filled circles) and C_{70} (filled triangles), and a comparison with the calculated heat capacity assuming that only vibrations contribute to the heat capacity of C_{70}. The heat capacity of $C_{70}\cdot C_6H_5CH_3$ was further adjusted by subtracting the heat capacity of solid and liquid toluene (below and above 178 K, respectively) (open triangles).

^{13}C NMR. Figure 3 shows typical powder patterns obtained without magic angle spinning for the $C_{70}\cdot C_6H_5CH_3$ and C_{70}. The measurements were carried out at the temperatures between the disordering transitions detected by the endotherms in the DSC traces (Figures 1 and 2). Each powder pattern for the $C_{70}\cdot C_6H_5CH_3$ in Figure 3 has been paired with a line representing the contributions from C_{70}. The additional up-field intensity (shaded areas) arises from the toluene. The MAS spectrum, obtained with single pulse excitation and without decoupling of protons, is plotted at the bottom to show the isotropic positions (chemical shifts) of the chemical shift anisotropy (CSA). A simulated powder-pattern is shown at the top to predict the CSA powder line-shape for *immobile* C_{70} molecules. The simulation is based on the assumption that the

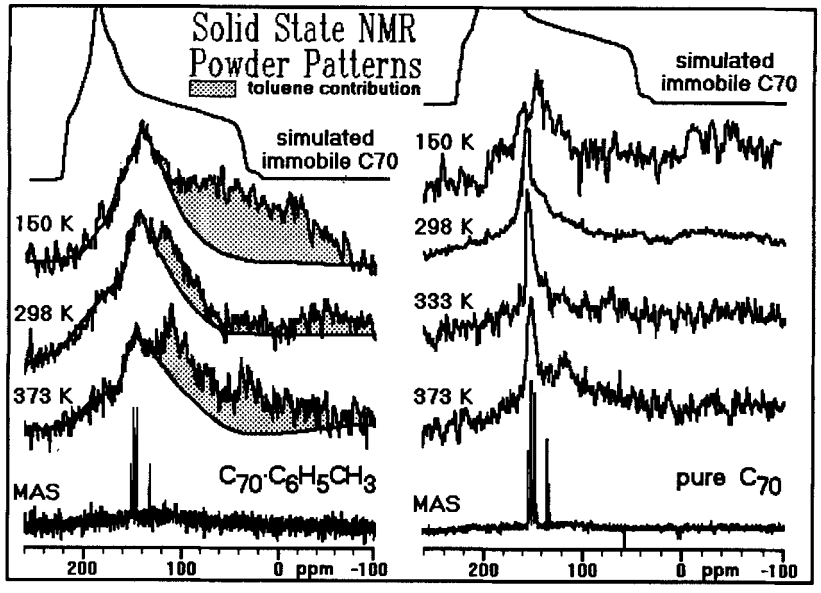

FIGURE 3 Solid state ^{13}C NMR (50.3 MHz) powder patterns of $C_{70}{\cdot}C_6H_5CH_3$ (on the left) and pure C_{70} (on the right) at the indicated temperatures. The smoothed spectra for the complex represent the contributions from C_{70}, while the upfield portions (shaded areas) arise from the toluene. The bottom curve represents a magic-angle-spinning spectrum obtained under the conditions of single pulse excitation and no decoupling of protons. The top plots are identical, simulated powder patterns for immobile C_{70} molecules, (for details see text, the peak position for the right set of curves can be judged from the left top plot).

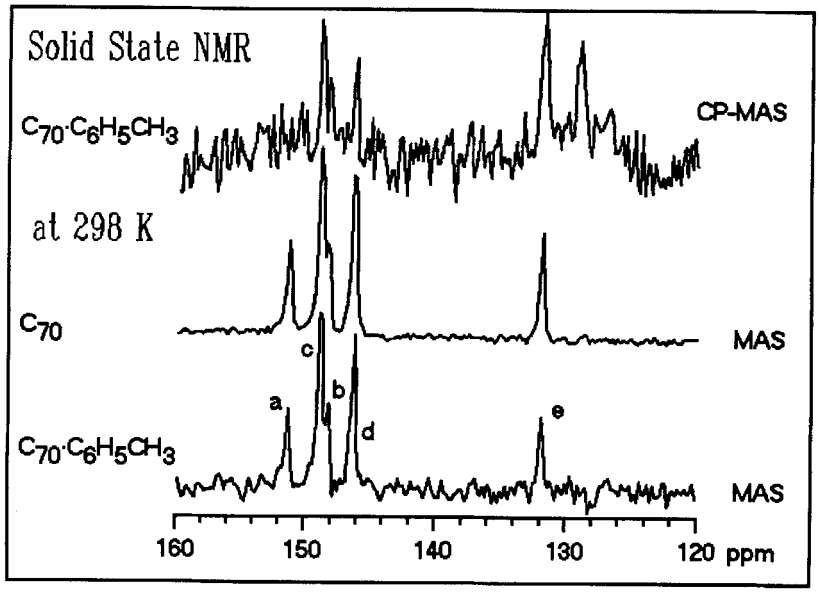

FIGURE 4 Solid state ^{13}C NMR (50.3 MHz) magic-angle-spinning (MAS) spectra. The top spectrum is of $C_{70}{\cdot}C_6H_5CH_3$ and was obtained with cross-polarization. The bottom and middle spectra are an expansion of the MAS spectra shown in Figure 3 and refer to $C_{70}{\cdot}C_6H_5CH_3$ and C_{70}, respectively.

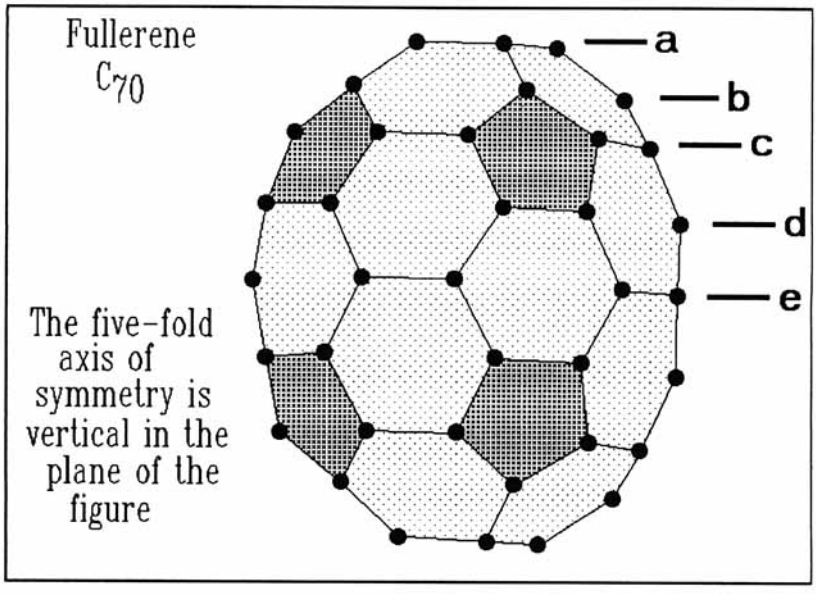

FIGURE 5 Molecular structure of C_{70}. The numbering of carbon atoms *a*, *b*, *c*, *d*, and *e* is used in Figures 3 and 4.

lineshape and the chemical-shift-anisotropy for all five distinguishable carbon atoms in C_{70} are the same as that for C_{60}, and on the knowledge of the isotropic chemical shifts shown by the MAS spectrum.

Figure 4 shows three spectra obtained with MAS at 298 K. The top spectrum is a CP-MAS spectrum of the as-received sample (complex), the bottom and middle spectra are the expansions of the bottom plots in Figure 3 (MAS spectra measured under the conditions of single pulse excitation without decoupling of the protons). The spectral difference between $C_{70}{\cdot}C_6H_5CH_3$ and C_{70}. (ie., between the middle and the bottom plots in Figure 4) is hardly noticeable.

The MAS spectrum shown in either the middle or bottom plot of Figure 4 consists of five lines at 151.3, 148.9, 148.2, 146.2 and 131.8 ppm, corresponding to carbon atoms *a*, *c*, *b*, *d*, and *e*, shown in Figure 5. The assignments can be made based on molecular structural determination in solution[6,7] and are in good agreement with all other reports for the C_{70} NMR spectra in the solid state.[4,5] The signal intensity of the peaks at 148.9 and 146.2 ppm is twice that at 151.3, 148.2, and 131.8 ppm, indicating that the number of carbon atoms at positions *c* and *d* is double that at positions *a*, *b*, and *e*.

DISCUSSION

Low Temperature Behavior of C_{70}

Measurements of the chemical shift anisotropy (CSA) powder patterns of C_{60} provide information on the orientational motion.[4,8,9] Below 100 K, where orientational

motion for most of the C_{60} molecules is quenched, the powder pattern of C_{60} shows the principal elements of the CSA tensor to be: $\sigma_{11} = 213$ ppm, $\sigma_{22} = 182$ ppm, and $\sigma_{33} = 33$ ppm. The isotropic position is thus $\sigma_{iso} = (\sigma_{11} + \sigma_{22} + \sigma_{33})/3 \approx 33$ ppm, which is observed, indeed, in the plastic crystalline phase ($T > 269$ K).[8] Notice, that there is a difference of about 40 ppm between σ_{22} and σ_{iso}.

For C_{70} the most intense point of the powder pattern is shown by the simulated spectrum to be at about 188 ppm for the immobile molecules (simulated spectrum in Figure 3). At the lowest experimental temperature of this NMR study (150 K), the spectrum for immobile molecules has still not been reached, although the powder pattern broadens considerably compared to those at higher temperatures. The most intense point in the measured spectrum at 150 K is located at about 145 ppm instead of 188 ppm, and the linewidth is much narrower than the simulated spectrum. Thus, the C_{70} molecules of both samples studied in this work are still mobile at 150 K.

The motion at such low temperatures is confirmed by the heat capacity analysis, in which the experimental heat capacity is still larger than that expected for solely vibrations contributing (see Figure 2). Freeze-in of the remaining disorder, and consequently a much more asymmetric and broader ^{13}C NMR powder pattern, are expected by further decreasing the temperature. The experimental and calculated heat capacities match at about 120 K, suggesting that below this temperature all loss of orientational entropy on cooling stops. If any large-amplitude motion is left, it would have to be jumps between positions of equal symmetry about the five-fold axis. A similar motion was observed in C_{60},[8,10] where the entropy loss stops gradually on reaching 190 K,[1] but a jump-like motion continues down to 100 K.[1,8,10]

Motion and Disorder of $C_{70} \cdot C_6H_5CH_3$

For the as-received sample, attempts have been made to reveal the signals from toluene after the existence of a complex had been proven by DSC and mass spectrometry. At room temperature and below, the resonances of toluene can not be observed with certainty (see Figure 3), presumably because the line-width of toluene molecules is too broad, due to the fact that neither the decoupling of protons nor MAS is applied to remove the hetero-nuclear dipolar interaction and chemical shift anisotropy, respectively. The presence of the toluene molecules in the complex is shown, however, by the spectrum of 373 K in Figure 3. There are two prominent features at 373 K in Figure 3 at about 120 and 40 ppm, corresponding to the resonances of protonated aromatic and methyl carbons, respectively. By knowing the approximate positions of toluene signals, one can trace them back to lower temperatures at 298 and 150 K. As can be seen, the signals of toluene become progressively broader with decreasing temperature. The toluene signals can also be detected by the CP-MAS method. The protonated aromatic carbon atoms of toluene appear at 129 and 126.8 ppm in the CP-MAS spectrum shown in Figure 4.

Turning to the DSC results of Figure 2 one can observe that: (a) the disordering transitions of the pure C_{70} are missing for $C_{70} \cdot C_6H_5CH_3$; (b) deviations from the purely vibrational heat capacity occur for both, the pure C_{70} and complex at about 120 K; (c) approximately above the melting temperature of pure toluene (178 K) the complex heat capacity can be represented only by the sum of the C_{70} heat capacity and

the *liquid* toluene heat capacity, i.e., the packing of the toluene in the complex seems to be similar to that in solid toluene, permitting large-amplitude motion at a temperature close to the melting temperature of toluene; (d) above the decomposition of the complex (after mass adjustment), the heat capacity of C_{70} reaches again the level expected for vibrations only; (e) the decomposition of the complex occurs 62 K above the boiling point of pure toluene with 2.9 kJ/mol higher enthalpy of transition than the heat of evaporation of one mole of toluene.

These observations can be interpreted as indicating that initial motion with gain in entropy occurs for both complex and C_{70} at about 120 K. Additional liquid-like mobility is achieved in the complex by the toluene at about 180 K. The change to a full plastic crystal seen in C_{70} between 261 and 338 K, does not occur in the complex, rather it continues developing its motional entropy as it did below these transitions (open triangles in Figure 2). Between 340 and 450 K the C_{70} molecules in the complex are, thus, still not in the plastic crystalline state with isotropic rotations. Only above the decomposition are both samples equal and correspond to the plastic crystal of C_{70}. Once the entropy of disordering (and change in crystal structure) is absorbed, the heat capacity does not deviate much from the vibrational heat capacity. Three degrees of freedom have changed from vibrational ($C_v = R$ per degree of freedom) to rotational ($C_v = R/2$ per degree of freedom), decreasing C_v by only $12\,JK^{-1}mol^{-1}$ or $0.015\,JK^{-1}g^{-1}$. Most of this decrease is, however, compensated by the expected higher expansivity of the plastic crystals, so that overall, no effect is seen within the experimental precision of about 2%.

Comparison of the NMR powder patterns of the complex and C_{70} in Figure 3 reveals that the former are much broader than the latter. Thus, the toluene molecules despite liquid-like mobility above 180 K hinder the orientational motion of the C_{70}, perhaps due to the fact that the overall shapes of toluene as well as C_{70} are non-spherical. In the presence of toluene, the C_{70} molecules are, however, still somewhat mobile since the width of the powder pattern shown in Figure 3 is narrower than that of the simulated spectrum for immobile molecules.

The ^{13}C NMR MAS spectra for the complex and C_{70} do not differ significantly at room temperature, as shown in Figure 4. Our results on the chemical shifts for all five different carbon atoms in C_{70} are the same as those reported for various C_{60}/C_{70} mixtures (the difference is no more than 0.1 ppm).[4,5] The identical chemical shift values of C_{70} and the complex implies, either that in $C_{70}\cdot C_6H_5CH_3$ the C_{70} molecules crystallize preferentially with other C_{70} molecules, or that the five resonance positions are only weakly dependent on the local molecular environment (packing). The former is not possible because it also implies that the toluene molecules would have to aggregate with other toluene molecules to form a liquid at room temperature, which contradicts the higher decomposition temperature and heat. Thus, the intermolecular influence on the chemical shifts (or the packing effect) must be negligible, which is particularly reasonable for C_{70} and toluene molecules that have orientational motion.

Possible Packing of C_{70} with Toluene

It is known that C_{70} molecules in the plastic crystalline phase have face-centered cubic (fcc) or hexagonal close packed (hcp) crystal structures, depending on the temperature,

crystallization conditions, and presence of foreign molecules.[3,11] Only at low temperatures are rhombohedral and monoclinic phases found. The fcc and hcp structures consist of equal number of large octahedral holes (formed by six neighboring C_{70} molecules) and C_{70} molecules, and double the number of small tetrahedral holes. Since the molar ratio between C_{70} and toluene is 1, and because of the larger size of an octahedral hole, it is reasonable to postulate that the toluene molecules in the complex occupy similar voids in the crystal below 470 K, i.e., we assume that the crystal structure (at present not known) can be related to the C_{70} plastic crystal by a loss of some rotational averaging and a corresponding decrease in symmetry.

From Figure 4, it is, furthermore, interesting to see that cross-polarization between the protons of toluene and C_{70} carbons is possible (i.e., the resonances of the C_{70} molecules are observable with the cross-polarization method). Because C_{70} has no protons, the cross-polarization must proceed by intermolecular transfer from the protons in toluene. This fact proves that the toluene molecules are mixed with the C_{70} molecules at the molecular level. With a pure C_{70} sample, the same CP-MAS experiment yielded no signal at all. Furthermore, the intensities of the five distinguishable carbon atoms in C_{70} do not follow the ratio of 10:10:20:20:10 for carbon atoms *a*, *b*, *c*, *d*, and *e*, as observed using single pulse excitation in Figure 4 or Figure 3. The resonance of carbon *e* (131.8 ppm), which is at the equatorial "belt", is most intense, and the signal for carbon *a* is absent. Since the cross-polarization efficiency in this case depends exclusively on the distance over which the hetero-nuclear (^1H–^{13}C) dipolar interaction occurs, the toluene molecule must be furthest from carbon *a* and the closest to carbon *e*. Assuming the C_{70} molecules are arranged with parallel five-fold axes, one can see that of the six C_{70} molecules forming the environment of the toluene molecule, four C_{70} must have their carbons *e* touching the toluene, while the other two have carbon *a* pointing at the toluene. The distance between the toluene and carbon *a* may, however, be longer than that between the toluene and carbon *e* of the C_{70}. Thus both the considerations of number of contacts and contact distances of toluene are in agreement with the CP-MAS spectrum in which the signals of carbon *e* is enhanced.

Details of the Motion and Disorder at Room Temperature and Above

The powder patterns of pure C_{70} are shown on the right side of Figure 3. At 298 K the resonance consists of a sharp symmetric peak at about 148 ppm with a less intense symmetric peak as a shoulder at about 130 ppm. The main peak is due to carbons *a*, *b*, *c*, and *d*, and the shoulder is from carbon *e*. The spectrum at 298 K for the pure C_{70} can be deconvoluted to consist of two symmetric lines with a linewidth of about 500 Hz (10 ppm), as shown in Figure 6. The linewidth is identical to that observed for C_{60}, but much less than that for the C_{70} in a mixture of C_{60} and C_{70}.[4] Using a slow sample spinning rate of 1 kHz, at least four spinning sidebands for C_{70} could be observed in Reference 4 for each carbon, indicating that the linewidth of the powder pattern (CSA) is at least 3 kHz instead of 500 Hz as observed in Figure 6. The difference between the observations in Reference 4 and in Figure 6 is perhaps due to the difference in the C_{70} samples, the former used a mixture of C_{60} and C_{70}, while no C_{60} could be detected in our sample. The fact that the spectrum has a symmetric line shape and a greatly reduced linewidth indicates that the molecules rotate rapidly and nearly isotropically. This is in

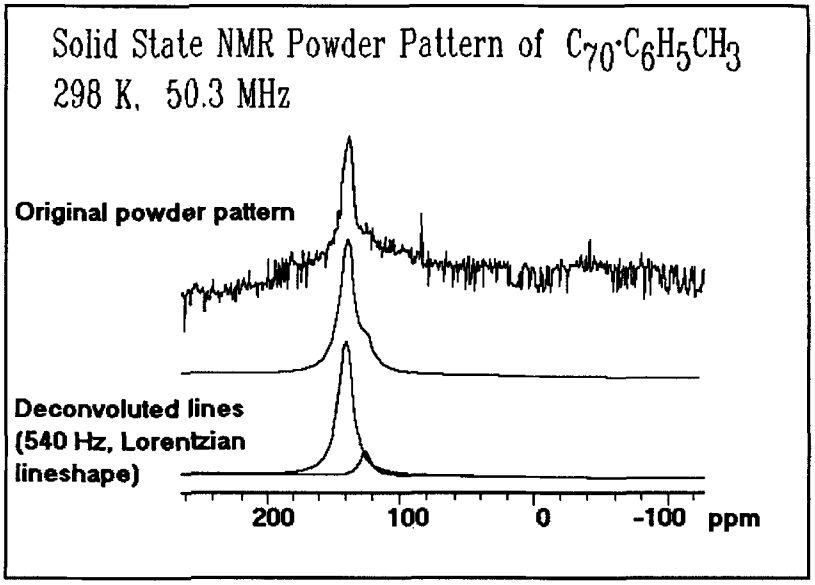

FIGURE 6 Top: solid state ^{13}C NMR (50.3 MHz) powder patterns of C_{70}·$C_6H_5CH_3$ at 298 K. Bottom: deconvoluted spectral lines using a line width of 504 Hz, and symmetric Lorentzian lineshape.

agreement with the conclusion made by Belahmer *et al.*, for a sample with 94% of C_{70} with about 6% of C_{60} based on the measurements of spin-lattice relaxation times.[5] The rotational correlation time must be short compared to the inverse of the CSA width, which is 110 μs. The spectra of the pure C_{70} obtained at 333 and 373 K in Figure 3 have a linewidth even narrower. The lower signal-to-noise ratio of the spectra at 333 and 373 K is due to a smaller number of averagings.

The C_{70} molecules in the C_{70}·$C_6H_5CH_3$ complex show a more complicated powder pattern (Figure 3). The lineshape appears to be more asymmetric with a linewidth of about 2300 Hz (45 ppm). This change in lineshape and linewidth as compared to that of the pure C_{70} is apparently caused by the toluene. Since the toluene molecules are near carbon *e*, as shown above, the rotation of the C_{70} molecules must most probably occur about the five-fold axis (long axis of the prolate ellipsoid). In fact, a spectral component centered at about 190 ppm is observed at 298 and 373 K in Figure 3, which might be the partial average of σ_{11} and σ_{22}. The rotation of C_{70} molecules about the short axes as it occurs in the pure C_{70} seems to be hindered because of lack of space in the filled interstices. That the motion is not completely stopped and increases as temperature increases, can be seen from Figure 3 where the average peak position approaches the isotropic peak position marked. Thus, in addition to a highly facile rotation about the long axis, increasing orientational motion about other molecular axes (short axes) can also occur. Consequently, the actual motion of C_{70} in the presence of toluene molecules is rather inhomogeneous and hindered, but considerable orientational disorder is evident.

Such gradually increasing disorder in C_{70}·$C_6H_5CH_3$ starting with rotation about the five-fold axis and spilling over to rotation about the short axes would easily account

for the observed increase in entropy starting at 120 K and continuing to the decomposition peak.

CONCLUSIONS

(1) Combing NMR and calorimetry, structural and motional information of pure C_{70} and C_{70} in the toluene complex could be derived. The structure is a physical 1:1 mixture of the molecules. The motion of the C_{70} molecules is restricted by the presence of the toluene.

(2) In the pure form, C_{70} molecules have nearly isotropic orientational motion at room temperature. The motion becomes more restricted at temperature of 150 K as the heat capacity approaches purely vibrational character. The beginning of full, isotropic motion seems coupled with two endothermic transitions.

(3) The position of the toluene in the complex $C_{70} \cdot C_6H_5CH_3$ is near the equatorial "belt" of the C_{70} molecule. The motion of the C_{70} is asymmetric, beginning with rotating about the molecular long-axis. The entropy increase is distributed without an observable endothermic transition between 150 K and the decomposition endotherm at 446 K.

(4) The toluene molecules seem to gain liquid-like mobility close to the melting temperature of pure toluene (178 K).

(5) The chemical shifts for all five distinguishable carbon atoms in C_{70}, which are indicated by the magic-angle-spinning spectra, are the same for pure C_{70} and the complex. In both cases the intermolecular contributions to the chemical shifts is unimportant because of the fast molecular orientational motion.

(6) In combination with the calorimetric data, one can conclude that the C_{70} in both samples forms plastic crystals of different dynamic orientational disorder. In case of the complex, the plastic crystalline state is reached more gradually.

Acknowledgments

This work was supported by the Division of Materials Research, National Science Foundation, Polymers Program, Grant # DMR 92-00520 and the Division of Materials Sciences, Office of Basic Energy Sciences, U.S. Department of Energy, under Contract DE-AC05-840R21400 with Martin Marietta Energy Systems, Inc. Part of work was also supported by Grant DE-FG05-88ER13859 from the U.S. Department of Energy, Office of Basic Energy Sciences, and by the cooperative agreement between the University of Tennessee and the Oak Ridge National Laboratory.

References

1. Y. Jin, J. Cheng, M. Varma-Nair, G. Liang, Y. Fu, B. Wunderlich, X. D. Xiang, R. Mostovoy and A. K. Zettl, *J. Phys. Chem.*, **96**, 5151 (1992).
2. Y. Jin, A. Xenopoulos, J. Cheng, W. Chen, B. Wunderlich, M. Diack, C. Jin, R. N. Compton and G. Guiochon, *Mol. Gyst. Liq. Cryst.*, submitted.
3. E. Grivei, B. Nysten, M. Cassart, J.-P. Issi, C. Fabre and A. Rassat, *Phys. Rev. B*, **47**, 47 (1993); see also G. B. M. Vaughan, P. A. Heiney, J. E. Fischer, D. E. Luzzi, D. A. Ricketts-Foot, A. R. McGhie, W. J. Romanow, B. H. Allen, N. Coustel, J. P. McCauley, and A. B. Snith III, *Science*, **254**, 1350 (1991).
4. R. Tycko, R. C. Haddon, G. Dabbagh, S. H. Glarum, D. C. Douglass and A. M. Mujsce, *J. Phys. Chem.*, **95**, 518 (1991).

5. Z. Belahmer, L Firlej, P. Bernier, A. Zahab, M. Ribet, N. Coustel and R. Aznar, *Extended Abstract of Symposium AA, Materials Research Society, AA5.39*, Boston, Massachusetts, Fall, 1992.
6. R. Taylor, J. P. Hare, A. K. Abdul-Sada, and H. W. Kroto, *J. Chem. Soc., Chem. Commun.*, **20**, 1423 (1990).
7. R. D. Johnson, G. Meijer, J. R. Salem and D. S. Bethune, *J. Am. Chem. Soc.* **113**, 3619 (1991).
8. R. Tycko, G. Dabbagh, R. M. Fleming, R. C. Haddon, A. V. Makhija and S. M. Zahurak, *Phys. Rev. Lett.*, **67**, 1886 (1991).
9. C. S. Yannoni, R. D. Johnson, G. Meijer, D. S. Bethune, and J. R. Salem, *J. Phys. Chem.*, **95**, 9 (1991).
10. R. D. Johnson, C. S. Yannoni, H. C. Dorn, J. R. Salem and D. S. Bethune, *Science*, **255**, 1235 (1992).
11. M. A. Verheijen, H. Meekes, G. Meijer, P. Bennema, J. L. de Boer, S. van Smaalen, G. van Tendeloo, S. Amelinckx, S. Muto and J. van Landuyt, *Chem. Phys.*, **166**, 287 (1992).